

## Article

# A Hybrid Control Path Planning Architecture Based on Traffic Equilibrium Assignment for Emergency

Zilin Zhao <sup>1</sup>, Zhi Cai <sup>1</sup>, Mengmeng Chang <sup>2</sup> and Zhiming Ding <sup>3,\*</sup>

<sup>1</sup> Faculty of Information Technology, Beijing University of Technology, Beijing 100124, China; zhaozilin@emails.bjut.edu.cn (Z.Z.); caiz@bjut.edu.cn (Z.C.)

<sup>2</sup> College of Computer and Information Engineering, Henan Normal University, Xinxiang 453007, China; changmengmeng@htu.edu.cn

<sup>3</sup> The Institute of Software, Chinese Academy of Sciences, Beijing 100190, China

\* Correspondence: zhiming@iscas.ac.cn

**Abstract:** Unconventional events exacerbate the imbalance between regional transportation demand and limited road network resources. Scientific and efficient path planning serves as the foundation for rapidly restoring equilibrium to the road network. In real large-scale road networks, especially during emergencies, it is usually difficult to obtain or predict accurate dynamic traffic network flows in real-time, which is used to support equilibrium path planning. Moreover, the traditional iterative methods cannot meet the real-time demand of emergency equilibrium path planning decision generation. To solve the above problems, this paper proposes a hybrid control architecture for path planning based on equilibrium traffic assignment theory. The architecture introduces the travelers' real-time travel data and constructs a spatio-temporal neural network, which captures the evolution of traffic network loads. Adaptive multi-graph fusion technology is used to mix the background traffic flow data and the traveler's real-time Origin–Destination (OD) data, to mine the dynamic correlation between the traffic state and the travelers' travel. Based on the real-time prediction of dynamic network states, equilibrium mapping learning is carried out to pre-allocate potential travel demands and construct equilibrium traffic graphs based on system optimization traffic assignment. Finally, individual evacuation path strategies are generated online in a data-driven manner in real time to achieve improved resilience in the transportation system.



**Citation:** Zhao, Z.; Cai, Z.; Chang, M.; Ding, Z. A Hybrid Control Path Planning Architecture Based on Traffic Equilibrium Assignment for Emergency. *Appl. Sci.* **2024**, *14*, 1253. <https://doi.org/10.3390/app14031253>

Academic Editor: José Salvador Sánchez Garreta

Received: 23 November 2023

Revised: 17 January 2024

Accepted: 29 January 2024

Published: 2 February 2024



**Copyright:** © 2024 by the authors. Licensee MDPI, Basel, Switzerland. This article is an open access article distributed under the terms and conditions of the Creative Commons Attribution (CC BY) license (<https://creativecommons.org/licenses/by/4.0/>).

**Keywords:** equilibrium assignment; background traffic; emergency recovery; spatio-temporal neural networks; path planning

## 1. Introduction

With the development of the economy, there are more and more vehicles in the urban road network. Traffic decongestion is increasingly becoming a daily challenge for urban traffic management. Especially in big cities where there are more people and cars, the road conditions are more complicated and there are often temporary emergencies (e.g., traffic accidents, temporary road control, and large events such as concerts and exhibitions). If the manager is unable to rapidly guide the vehicle to modify the route to guide the traffic to achieve a balanced state, it will make the local congestion continue to spread, thus affecting the smooth flow of the large area of the road network. Such temporary emergencies are unpredictable, accidental, and irregular. After an emergency, it is crucial for the system to be able to calculate and adjust the travelers' planned routes in time and guide the transportation system to rapidly return to the original traffic equilibrium [1]. Traffic equilibrium means that no traveler in a transportation system can unilaterally reduce his travel impedance by changing his path [2]. Existing traffic forecasting and route planning methods make it difficult to meet the actual needs of prediction accuracy and decision-making efficiency in such emergency scenarios.

Firstly, the impact of such emergencies on the traffic state is affected by the local road network structure and the activities of the surrounding travelers, which makes it difficult to devise a generalized method for prediction. Traffic equilibrium is one of the main research objectives in traffic assignment modeling and route planning, which has already produced more results [3–5]. For example, the static traffic assignment (STA) typically assigns the current real-time origin–destination data (OD) used, such as Logit probabilistic stochastic methods [6–9], to estimate the road impedance, which can quantify the impact of real-time OD on the road network. However, the traffic on the entire road network changes dynamically. Such static methods are difficult to adapt to the real road network at the time of emergencies. In addition, in reality, information on accurate and dynamic road network traffic flow is usually difficult to obtain in real time. Existing dynamic traffic assignment (DTA) studies usually depict the dynamic distribution of traffic flows based on linear or constant different metrics [10–13], optimization objectives [14], or probabilistic approaches [15]. But because many factors are difficult to quantify in emergencies, it is difficult to describe the complex and variable dynamic traffic flow distribution relying only on simple variables or probability distributions. Therefore, route planning after an emergency should consider not only real-time traveler OD information (referred to as micro-information), but also real-time and future information about the overall background traffic flow (referred to as macro-information). We concluded that it is difficult to consider either micro or macro transportation information in isolation to achieve accurate prediction and planning after an emergency event.

Second, in terms of model performance, while existing flow allocation models are well structured and reasonably well explained, they often imply a large number of variables and constraints. The solution algorithms are often computed iteratively by constantly choosing the optimal path. Only after continuous adjustment within the system can the algorithm reach an equilibrium state. Due to the excessive number of iterations, the computation time of these algorithms is too long, and the ability of real-time planning and decision-making is greatly reduced. And the re-planning of travelers' routes in emergency scenarios requires high algorithm performance for real-time decision-making. The traditional iteration-based approach is difficult to adapt to this rapid planning and decision-making requirement.

In summary, how to be able to rapidly and accurately re-route and guide the traffic back to equilibrium after an emergency is a key issue facing traffic relief. The main contributions of this paper are as follows:

- (1) A hybrid control architecture that combines network-wide traffic flow data (macro information) and travelers' real-time OD data (micro information) is proposed, which provides the system with emergency-compatible and more accurate real-time traffic load for dynamic road networks.
- (2) A spatio-temporal neural network-based traffic equilibrium assignment model (ST-ETA) is given, mapping the equilibrium assignment aiming at system optimization (SO) into a neural network. The problem of real-time path planning for emergency scenarios in large-scale real road networks is solved by learning the mapping relationship between the current traffic condition and the optimal equilibrium distribution, instead of an iterative approach.

The beginning of this paper lists the current research related to path planning based on traffic assignment and traffic forecasting. The second part will briefly describe the principles of equilibrium traffic assignment and the theoretical basis for hybrid control path planning. The third section details the hybrid control architecture. In the fourth part, a series of experiments and result analysis are given to verify the model validity. In the last part of this paper, we conclude and put forward the future research work.

## 2. Related Work

### 2.1. Path Planning Based on Traffic Assignment

The research community has proposed various techniques to improve path planning in emergencies using traffic assignment methods. Earlier, researchers used the static traffic as-

signment (STA) [6–9] to estimate road impedance conditions and guide traveler assignment. For example, the Logit assignment model [5] is a typical probabilistic stochastic assignment method that assumes that the user's error in estimating the actual road impedance satisfies a Logit distribution. However, the period of traffic distribution is difficult to determine. If the interval is short, the traffic state will be affected by the previous period, and vice versa, it will change drastically. This is because static models do not reflect dynamic changes in traffic states. This has led to a shift in the study of traffic assignment to the more realistic dynamic traffic assignment (DTA) [16]. DTA focuses on discovering the natural evolution of the transportation system and thus depicts the continuous distribution of traffic flows [17]. DTA has been favored by various works for its typical application in congested networks such as frequent emergencies [18–20]. Several researchers have proposed different DTA-based techniques to estimate and depict the continuous distribution of traffic flows and in the process accomplish path planning. Pel et al. presented a review of travel behavior modeling in dynamic traffic simulation models of evacuation from four aspects [10]: traveler behavior, travel demand, trip distribution, and traffic assignment representation. In addition, [21,22] and others have also studied the DTA problem through real-time traffic simulation. Ref. [11] optimized the traffic distribution using the method of successive averaging (MSA) and solving the dynamic equilibrium problem for UEs and SOs using the time-varying shortest path algorithm. The MSA method is also used in [12]. The authors additionally utilized Mahut's temporal queuing method [23] to solve the path runtime computation, which improves the computational efficiency. These two studies are based on simulated small-scale road network models, and it can be seen that MSA will be extremely inefficient in large-scale transportation networks due to its iterative computational approach.

Subsequently, some researchers have started to consider the impact of real transportation network evolution on path planning. Di Gangi [13] proposed an extension to a mesoscopic dynamic traffic assignment (DTA) model which was developed to determine quantitative indicators for estimating the exposure component of the total risk incurred by the transport networks in an area. But the method's deterministic assessment using linear or constant metrics does not express the complex dynamics of transportation well. Ref. [24] proposed an equilibrium model considering dynamic background traffic flow in a problem targeting parking lot evacuation optimization, and experimentally demonstrated that the background traffic flow has a great influence on the selection of the optimal path. Then, Tao Zhang [14] clearly defined the concept of background traffic, i.e., the traffic flow consisting of existing vehicles on a road network before emergency evacuation affects the assignment of evacuation vehicles, consequently affecting the formulation and implementation of emergency plans. In this work, they considered the presence of background traffic in dynamic evacuation traffic studies based on three constraints, including the state equation, propagation function, and conservation. Experimental validation by [14,24] shows that background traffic is an important guide for the generation of traffic assignment strategies.

However, while some of the above work also attempts to give real-time path planning decisions by determining the evolution of traffic flows, the evolution of network traffic predicted by the model is usually only applicable to deterministic scenarios. Emergencies have considerable uncertainty. However, while some of the above work attempts to give path-planning decisions by judging the evolution of traffic flows, the evolution of network traffic predicted by the model is usually only applicable to deterministic scenarios, since emergencies have considerable uncertainty [15]. Individuals are likely to change their established routes when faced with unforeseen circumstances, which leads to the failure of traffic prediction models backed by normative data. To address this problem, Di Gangi uses a probabilistic approach to directly predict the time evolution of the probability of evacuating users from an area. But individual rerouting behavior is directly affected by the metrics selected for generating the probabilities, and we cannot judge the merits of the metric selection. Moreover, the probabilities are generated in different emergencies in different ways. Therefore, how to consider the impact of individual trips on macroscopic

background traffic flow, so that the model can compatibly predict future background traffic in the existence of anomalies, and thus support the traffic assignment work in real-time becomes the focus of our work.

To assess the impact that micro individual demand brings to macro traffic flows, Ref. [25] quantified the impact of urban logistics activities on traffic flow dynamics through simple metrics of the macroscopic fundamental diagram (MFD) to investigate the possible benefits of multi-use lane strategy deployment. Ref. [26] proposed a framework for simulating micro freight demand through a probabilistic generation approach, and combined traffic states with stochastic and microscopic freight demand generation models, i.e., the delivery movements and the delivery duration. The intention is to use MFD and its associated metrics to capture and quantify the macro impacts of double-parked vehicles transporting goods on urban arterials. But both of these works are based on MFD. The macroscopic information in MFD is the impact of the relationship between the three main parameters of the transportation system, namely flow, speed, and density [27], rather than the impact on the network-wide traffic flow data. Furthermore, [28] formulated the dynamic OD demand estimation problem as an excess-demand dynamic traffic assignment (DTA) problem defined for an expanded network with dummy paths, and assumed that the network equilibrium is a compromise between minimizing the individual routing cost, traffic count matching error, and the OD demand entropy. Inspired by this work, we introduce travelers' real-time OD data to improve the prediction of dynamic traffic flows.

In summary, background traffic is an important guide for the generation of traffic-assignment strategies in emergencies. However, existing models use quantitative indicators, constraints, or probabilistic methods to predict background traffic, which cannot be adapted to equilibrium path planning in emergencies. In addition, existing allocation methods use iterative computation, which is extremely inefficient in large-scale traffic networks and cannot make real-time decisions. Therefore, in this paper, we combine the background traffic flow data and the traveler's real-time OD data to predict the accurate traffic network state under the influence of real-time OD, and further offer hybrid control of the traveler's path planning strategy. Moreover, the neural network mapping traffic assignment method is used instead of the iterative approach to enhance the real-time performance of the algorithm.

## 2.2. Traffic Prediction Based on Spatio-Temporal Neural Networks

The spatio-temporal neural networks have been widely applied in the traffic speed, traffic flow, travel demands, and traffic map predictions. Ref. [26] proposed an innovative method for predicting a dynamic OD matrix in a subway network using long short-term memory (LSTM) by analyzing the swipe data of subway passengers. This method cannot be directly applied to road network OD prediction due to the relatively fixed subway lines and the small scale of the subway network. Ref. [29] investigated the spatio-temporal dependence of ODs and proposed a multi-perspective graph convolutional network. The temporal features and spatial dependencies were extracted for each OD pair using LSTM and a two-dimensional graph convolutional network. Most taxi OD prediction methods only considered the demands at origin ignoring the destination the taxi arrived at. Ref. [30] proposed a contextualized spatio-temporal network to predict the future interactive demands between all regional ODs. Ref. [31] adopted tensor data to characterize OD streams and proposed a multi-scale convolutional LSTM to handle high-dimensional travel features by tensor permutation and matrixing. To alleviate OD data sparsity, Ref. [32] used a grid partition method dividing the road network to explore the correlation of ODs. This model combines geographic and semantic neighborhoods, with the geographic domain measuring the intrinsic closeness of grids and the semantic domain modeling the intensity of traffic between grids. Ref. [33] proposed a spatio-temporal residual neural network to predict the inflow and outflow of ODs in each region based on temporal closeness, period, and trend features. The ST-ResNet aggregates the outputs of three residual networks and

allocates different weights to different branches and regions, further combining the weather factor to predict the regional traffic.

The time-varying traffic flow of road sections is another perspective that reveals the evolution of traffic network, and real-time traffic flow prediction is the core issue in ITS. In previous traffic flow prediction, time series models were used to capture the autocorrelation between traffic statuses [34,35]. Subsequently, graph topological features were introduced to fit the spatial dependence of traffic flow [36]. Considering the complicated topological connectivity and nonlinear temporal dynamics of traffic context, Ref. [37] proposed a diffusion convolutional recurrent neural network. It captures the spatial correlation using bidirectional random walks on the graph and temporal dependence using the code-and-decode architecture. To improve the generality of convolution, Ref. [38] proposed a spatio-temporal graph convolutional network that simultaneously extracts spatio-temporal features from time-series graphs. It models the spatial features of the traffic network using general graph and adopts fully convolutional layers on the time axis. Ref. [39] extended the existing graph convolutional networks and proposed a novel graph-based neural network that distinguishes the intensity of connections to adjacent nodes revealing the hidden features of traffic propagation. To cope with the constraints of topology and the dynamic changes in traffic, Ref. [40] proposed a temporal graph convolutional network, which learns the complex topology to capture the spatial dependence, and extracts the dynamic temporal dependence of traffic. In the temporal dimension, the status feature in the distant past is not necessarily less important than the recent feature. Ref. [41] proposed an attentional temporal graph convolutional network that captures both global temporal dynamics and spatial correlation, which introduces an attentional mechanism to adjust the importance of different time series. Most of the existing graph convolution methods only consider local spatial correlations, but non-local associations are equally important. To obtain the non-local spatio-temporal features, Ref. [42] proposed a global spatial-temporal network to extract local and global spatial features.

In summary, the spatio-temporal neural network technique provides new theoretical support for dynamic traffic network flow with real-time prediction. Among them, graph convolution shows excellent ability in spatial trend feature extraction. In this paper, a spatio-temporal neural network is constructed that uses hierarchy graph convolution to capture the global traffic state as well as the potential traffic generated from the real-time OD data, so as to provide accurate and comprehensive real-time traffic load to the equilibrium path planning decision by traffic prediction.

### 3. Preliminaries

#### 3.1. Dynamic Road Network and Traffic Equilibrium Principle

A generalized dynamic road network  $G = (N, R, O^T, V^T)$  is obtained by combining the road network topology and the travelers' trajectories. The OD evacuation volume  $O^T$  and background load  $V^T$  change dynamically with the period  $T$ . The origin and destination of the OD come from two nodes in set  $N$ . The set of road sections in the network is denoted by  $R$ . We refer to the connection from the origin to the destination as the OD path  $l$ . The  $l$  consists of a series of adjacent link sequences  $\langle r_o, r_i, \dots, r_d \rangle$  which correspond to the road sections in the road network. Meanwhile, as the traffic load changes, the impedance of the road section varies simultaneously, and we use an evacuation time function to measure it.

**Definition 1 (Traffic Load).** *The total traffic volume carried by the road network during the time period, including background traffic flow loads (background load) as well as assigned evacuation volumes. The total traffic volume allocated to each section is called the traffic load of that section, and the maximum traffic load is equal to its capacity. Therefore, the real-time traffic load combined with the section capacity can be used to calculate the actual capacity.*

**Definition 2 (Travel Impedance).** *For the edge  $r_i$  in the OD path, the  $\delta(r_i)$  denotes the evacuation time cost function. The travel impedance for  $r_i$  can be expressed in Equation (1).*

$$C(r_i) = \{\delta(r_i) | \langle r_i \rangle \in l\}. \tag{1}$$

The travel impedance of path  $l$  is the total cost of the containing road sections, as in Equation (2):

$$C(l) = \delta^{(t_0)}(r_o) + \delta^{(t_1)}(r_i) + \dots + \delta^{(t_k)}(r_d). \tag{2}$$

where  $t_0, t_1, \dots, t_k$  denote the discretized time points, and  $k$  means the time steps spent on  $l$ .

In the evacuation of ODs, the travel impedance of the pre-planned path may increase due to the traffic load changes. The increasing traffic load on the path causes the pursuit of minimum evacuation costs  $C(l)$  to be invalidated, while some sections with low flow traffic are not fully utilized. The problem domain for hybrid control path planning is based on the criteria that the total evacuation cost of all ODs in the traffic network is minimized. The principle of system optimization for traffic assignment is used here.

**Definition 3 (System Optimization, SO [2]).** *With the constraint of traffic load balancing, traffic flows in a congested network should be assigned at the lowest average or total evacuation cost.*

The SO requires travelers to accept the system’s unified scheduling, where there is a collaborative relationship between them. Ref. [3] constructed a mathematical model to achieve system optimization under constraints, and regarded the OD flow as an equilibrium distribution of the network. This objective optimization function is shown in Equation (3).

$$\begin{aligned} \min z(L, V_L) &= \sum_{r_i \in L, v_{r_i} \in V_L} v_{r_i} C(r_i) \\ \text{s.t. } V_L &= \sum_{l \in L} \sum_{r_i \in l} v_{r_i}^l, v_{r_i}^l \geq 0 \end{aligned} \tag{3}$$

The  $z(\cdot)$  is the sum of the product of travel impedance and traffic load, and its optimal solution minimizes the function value. The constraints include the conservation of traffic between OD paths and road sections with non-negative section traffic. The  $V_L$  denotes the traffic volume of all OD paths  $L$ , and  $v_{r_i}^l$  denotes the traffic load of  $r_i$  in  $l$ . As the Beckmann-based traffic assignment methods use stepwise approximation, they are difficult to apply in large-scale traffic networks with high real-time requirements [43]. In this paper, we design and map the equilibrium traffic assignment method to data-driven deep learning, which is based on SO ideas for online real-time decision-making in large-scale transportation networks.

### 3.2. Formulation of Hybrid Control Path Planning Problem

Hybrid control path planning is a path decision model that combines network-wide traffic flow information (macroscopic information) and travelers’ real-time OD information (microscopic information) to consider traffic system optimization. In the path-planning process, it considers both individual paths cost  $C(l)$  and system cost  $z(L, V_L)$ . This is achieved by mapping the traffic equilibrium assignment method based on SO. However, background traffic flows at the macro level are not available in real time. Traffic assignment is only based on the macro background traffic flow, which cannot adapt to the situations wherein individuals change the established route to adapt to time-varying transportation system states in emergencies. Thus, the hybrid control path planning relies on the data-driven deep learning approach to perceive future traffic evolution.

We use the discrete time points  $(t - m, \dots, t - 1, t)$  to record the OD volume and background load of road sections. The prediction of the dynamic traffic load can be considered as learning the mapping function  $f(\cdot)$  based on  $O^T$  and  $V^T$ , as shown in Equation (4).

$$(o_r, v_r)^t = f \left\{ \tilde{A}; \begin{bmatrix} o_r^{t-m}, & \dots, & o_r^{t-1} \\ v_r^{t-m}, & \dots, & v_r^{t-1} \end{bmatrix} \right\}. \tag{4}$$

The  $o_r^t \in O^T$  denotes the OD volume and  $v_r^t \in V^T$  denotes the traffic load of node  $r$  at time  $t$ . The  $\tilde{A}$  is the spatial connectivity of the nodes in the road network. The historical data of  $o_r$  and  $v_r$  from  $t - m$  to  $t - 1$  can be represented as  $(o_r^{t-m}, \dots, o_r^{t-1})$  and  $(v_r^{t-m}, \dots, v_r^{t-1})$ . Considering that acquiring OD data is limited for some nodes, the historical data for  $o_r$  can be taken from other nodes with similar spatial patterns [44]. The traffic equilibrium graph can be considered as a priori traffic distribution of  $O^T, V^T$ . The traffic distribution  $F$  in period  $T$  has the following decomposition equation according to the conservation of traffic flow:

$$E(O^T, V^T) = (F_o^T |_{\min z(\cdot)}) + F_v^T. \quad (5)$$

Equation (5) learns an equilibrium distribution function  $E(\cdot)$  based on the SO-constrained traffic equilibrium assignment method that assigns OD evacuation volume to road sections. The hybrid control path planning builds upon the equilibrium distribution  $E_{(o,v)}^T$ , which equals finding a path with the largest potential traffic assignment. On this basis, the system recommends that path planning prioritizes using the road sections with potential traffic, which can reach a compromise between individual cost and system optimization, as shown in Equation (6):

$$l'_{(r_o, r_d)} = HRoute(r_o, r_d | r_i \in E_{(o,v)}^T). \quad (6)$$

where  $l'$  is the decision path under hybrid control. To capture the impact of dynamic traffic network for path planning, this paper attempts to learn a  $HRoute(\cdot)$  function that considers the overall traffic evolution trend of the system to the path planning of the individual traveler. In fact, the potential traffic assignment can better represent the evolution of the traffic network. Therefore, the hybrid control path planning model extracts the evolution features of the traffic network to calculate the individual paths.

#### 4. The Proposed Hybrid Control Architecture for Path Planning

Traffic allocation is based on dynamic traffic states and real-time OD states. In reality, network-wide traffic flow data cannot be collected and uploaded promptly, and equilibrium path planning decisions based on macro real-time traffic states are iteratively generated, both of which lead to scheduling delays. To meet the real-time requirements of path planning, on the one hand, the dynamic traffic load state can be foreseen by deep learning prediction, which combines the OD evacuation volume and background traffic flow. On the other hand, mapping SO constrains the traffic equilibrium-assigned method by the neural network approach. The path plan is given in real time based on the predicted traffic state and real-time OD data, so as to improve the effectiveness and timeliness of the traffic allocation. The hybrid control architecture for path planning named equilibrium traffic assignment based on spatio-temporal neural network (ST-ETA) can be subdivided into the dynamic traffic network load prediction module and the hybrid control path planning module, as shown in Figure 1. Among them, the feature extraction and prediction mechanism of the dynamic traffic network load prediction module corresponds to Sections 4.1 and 4.2, respectively. The hybrid control path planning module corresponds to Sections 4.3.

Considering the strong spatio-temporal correlation of OD volume or background load of the road network under discrete periods, our model assumes that we can estimate the evacuation volume for a given period by making a prediction based on the travelers' route data. And the dynamic road impedance on each section can be pre-calculated by predicting the future traffic load. The OD evacuation volume prediction module and the background traffic load prediction module are trained in parallel to capture OD trend features and background traffic flow change features, respectively. The equilibrium mapping layer fuses the two types of data to form a complete traffic flow distribution and captures the mapping relationship between this distribution and the optimal traffic equilibrium flow distribution. Ultimately, the optimal equilibrium flow distribution graph calculated from the real-time information is used as the basis for the path plan.

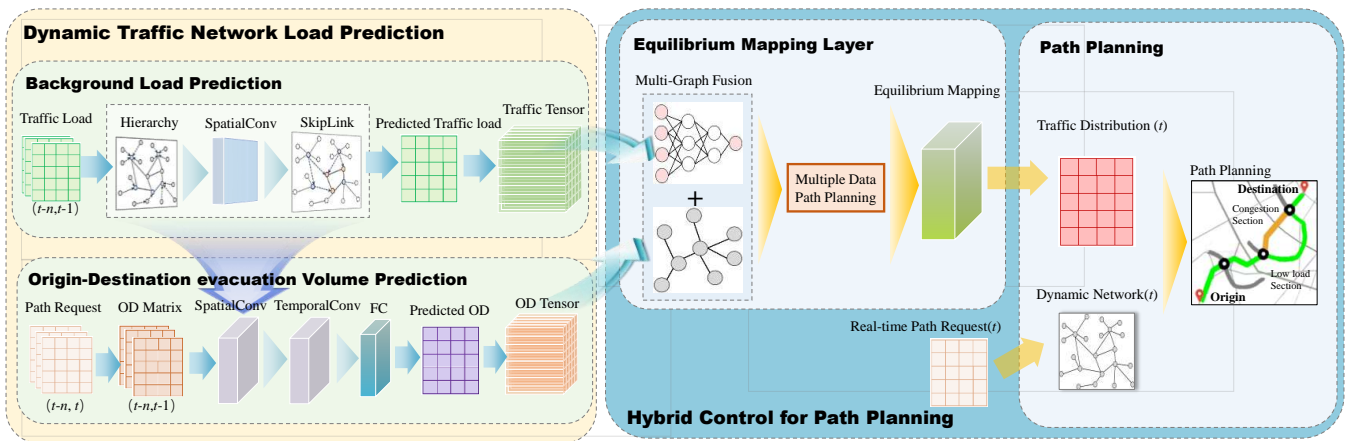


**Figure 1.** The hybrid control architecture for path planning based on equilibrium traffic assignment.

#### 4.1. Spatial Feature Extraction Based on Hierarchy Graph Convolution

To extract spatial features of OD and background load, we uniformly adopted a hierarchy graph convolution. The real-time OD data are then counted for each network node by time slices to form the OD evacuation volume. With the time dimension, the OD evacuation volume carries real-time spatial trend information.

The graph convolutional networks have been widely applied to extract spatial features in status snapshots of traffic network [38,40]. The topology of the traffic graph can be well portrayed by the Laplace matrix. The first-order Chebyshev graph convolution [45] simplified as  $\Theta * x \approx \theta(\hat{D}^{-\frac{1}{2}} \hat{A} \hat{D}^{-\frac{1}{2}})x$ , where  $\theta(\hat{D}^{-\frac{1}{2}} \hat{A} \hat{D}^{-\frac{1}{2}})$  is the approximating convolution filter,  $x$  is the input feature. Thus, the traffic status of one node in the road network can be treated as an aggregation of surrounding traffic. The perception field of the graph convolution can be expanded by stacking multiple GCNs embedded in the network. The feature transfer between the GCN layers is as in Equation (7):

$$H^{(l+1)} = \Gamma^{(GCN)}(\hat{D}^{-\frac{1}{2}} \hat{A} \hat{D}^{-\frac{1}{2}} \cdot H^{(l)} \cdot \Theta^{(l)}). \quad (7)$$

$H^{(l)}$  denotes the output vector of the  $l$ -th layer, and  $\Gamma^{(GCN)}$  is the ReLU activation function for performing the first-order spectral convolution. The GCN layer finally converts the input traffic background flow or OD evacuation volume  $X^t = (x_1^t, \dots, x_{i-1}^t, x_i^t)$  into a code  $H^t = (h_1^t, \dots, h_{i-1}^t, h_i^t)$ .

In a real road network, due to the complex connectivity of geographic space, it is not enough to explore the intrinsic relationships and regularities from the individual features of the nodes [46]. The network nodes form the OD volume matrix have extremely high dimensionality. It records all node-to-node traffic volumes. Since some intersections are low-level and often have no vehicles passing through them, the OD data are extraordinarily sparse, which usually makes it difficult to capture the effective trend characteristics carried by real-time OD. Moreover, it is impractical to use such a fine-grained road network to analyze and calculate traffic features. The spatial features can be further aggregated by semantic information and described in a coarse-grained manner.

The grid partition is a commonly used method for coarse-grained road network analysis, but the equidistant grid scales tend to disrupt the semantic relationships of the roads. The contraction hierarchy [47] generates a hierarchy structure by iteratively merging the lower ranked nodes in the road network. The contraction process is continuously adding the shortcuts to the edge set, and finally obtaining an overlay graph  $G_{\uparrow} := (N_{\uparrow}, R_{\uparrow})$  that preserves the shortest path feature of the original graph. After the coarse-grained contraction of the road sections, the traffic graph structural complexity and connection sparsity were improved. Furthermore, we encoded the coarse-grained spatial features based on the overlay graph  $G_{\uparrow}$  through the hierarchy graph convolution and skip graph



convolution, as shown in Figure 2. The neurons represent links in  $G_{\uparrow}$  and their activation statuses correspond to their traffic. The weight on the link can be interpreted as the probability of traffic assignment. The hierarchy features of nodes in  $G_{\uparrow}$  are encoded using graph convolution for the node that can be contracted. The hierarchy convolution network (HCN) first encodes the graph features with the correlation between shortcuts and edges, which can be defined as

$$Z^{(c)} = \Gamma^{(HierarchyConv)} (\hat{D}_c^{-\frac{1}{2}} \hat{C} \hat{D}_c^{-\frac{1}{2}} \cdot Z \cdot \Theta^{(c)}). \tag{8}$$

where  $Z \in \mathbb{R}^{n \times n}$  is the contraction matrix and  $Z^{(c)}$  is the output given by hierarchy convolution. Next, we perform neighborhood features extraction based on the shortcuts in  $A_{\uparrow}$ . The shortcuts are the coarse-grained description of the road sections, and we encode the adjacent relationships of shortcuts in  $G_{\uparrow}$ , as follows:

$$Z^{(h)} = \Gamma^{(SkipConv)} (\hat{D}_{\uparrow}^{-\frac{1}{2}} \hat{A}_{\uparrow} \hat{D}_{\uparrow}^{-\frac{1}{2}} \cdot Z^{(c)} \cdot \Theta^{(h)}). \tag{9}$$

where  $Z^{(h)}$  is the output of the skip convolution. Considering the prediction for multi-graph snapshots, we generate a sequence of hierarchy graph encodings  $Z^T = \{Z^{t-m}, \dots, Z^t\}$  by fusing spatial features of  $X^T = \{X^{t-m}, \dots, X^t\}$  through the HCN layer.

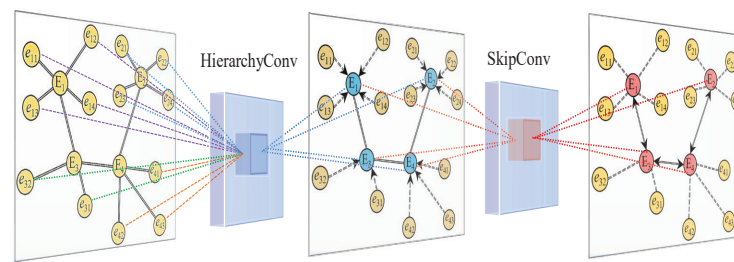


**Figure 2.** The process of extracting hierarchy features based on  $G_{\uparrow}$ .

#### 4.2. Dynamic Traffic Network Load Prediction

The objective of dynamic traffic load prediction is to capture the spatial and temporal evolutionary features based on historical data  $\{O_q | q = t - m, \dots, t - 1\}$  and  $\{V_q | q = t - m, \dots, t - 1\}$  to predict the evacuation volume  $o^t$  and background load  $v^t$ . In Section 4.1, we have extracted the spatial features for both data. For the temporal dimension, we have used the classical LSTM for both types of data. It takes  $o_t$  or  $v_t$  as input, and the output layer is processed by the internal memory cell to generate the  $h_t^o$  or  $h_t^v$  as input to the next cell.

In time series, the background load shows a recent, daily, and weekly periodical pattern [48]. Unlike background load prediction, the OD evacuation volume prediction is not closely related to the recent features. If evacuation features are consecutively extracted, the model captures the interference features which are not helpful for prediction in a compulsory manner [32]. Hence, we construct a coarse-grained prediction method that skips irrelevant sequences based LSTM to predict OD evacuation volume.

Based on the gate control units of LSTM, we designed a coarse-grained prediction model with multi-level memory that skips irrelevant sequences. The memory unit processes the input vector  $o_t, v_t$  through the forget gate, input gate, and output gate, respectively. And the output  $\Pi_t^{(o)}, \Pi_t^{(v)}$  of hidden layers via the activation function of gate is updated as shown in Equation (10):

$$\begin{aligned} \Pi_t^{(o)} &= \Gamma^{(gate)} (W^{(o)} [o_t, h_{\tau(t)}] + b^{(o)}), \\ \Pi_t^{(v)} &= \Gamma^{(gate)} (W^{(v)} [v_t, h_{t-1}] + b^{(v)}). \end{aligned} \tag{10}$$

where  $\tau(t)$  is the time period after the coarse granularity process. The  $W^{(o)}, W^{(v)}$  are the weight matrix of the input layer to the gates, and  $b^{(o)}, b^{(v)}$  are the corresponding bias. The

$\Gamma^{(gate)}$  is the sigmoid activation function. The OD's latent encoding of gate control units is computed using the embedding  $o_t$  and the hidden state  $h_{\tau(t)}$ . And the background load latent encoding is computed with  $v_t$  and  $h_{t-1}$ . The input gate and forget gate are used to update the cell state  $C_t$ , and the  $H'_t$  is controlled by the output gate and the activation unit, as in Equation (11):

$$\begin{aligned} C_t &= \Pi_t^{(forget)} \odot C_{t-1} + \Pi_t^{(input)} \odot \text{Tanh}(W^{(c)}[X'_t, H'_{t-1}]), \\ H'_t &= \Pi_t^{(output)} \odot \text{Tanh}(C_t). \end{aligned} \tag{11}$$

where  $\odot$  is the Hadamard product. The  $X'_t, H'_{t-1}$  come from the OD prediction of  $o_t, h_{\tau(t)}$ , or the traffic load prediction of  $v_t, h_{t-1}$ . Furthermore, the temporal encoding is converted in parallel by HCN to increase the depth of LSTM spatio-temporal contextual memory. The final output  $H^{(t)}$  is composed of the contraction encoding  $Z$ , temporal encoding  $H'_t$ , and spatial correlation  $\hat{C}, \hat{A}_{\uparrow}$ , as shown in Equation (12).

$$H^{(t)} = \Gamma^{(gate)}(\text{HCN}(Z, \hat{C}, \hat{A}_{\uparrow}), H'_t). \tag{12}$$

### 4.3. Path Planning Constrained by Equilibrium Traffic Assignment

To make the path planning constrained by the equilibrium traffic assignment, we first train a mapping layer to obtain the equilibrium graph. The path planning makes the routing decision based on the road sections with potential traffic. Therefore, finding the equilibrium traffic graph in the period to guide path planning can induce the traffic network to equilibrium. We propose a data-driven deep learning solution to derive equilibrium traffic graphs, as shown in Figure 3.

In the offline training phase, the SO-based traffic equilibrium sample generator uses the equilibrium graph obtained by the traffic assignment method to label the input traffic statuses, which provides data samples for the network training. The equilibrium mapping layer first obtains the joint traffic state distribution of ODs and background load, and then learns the mapping to the equilibrium graph based on the generated samples. The data-labeling process generates sufficient traffic distribution samples for the training of the equilibrium mapping layer. After offline training, the mapping module can perform online prediction and periodically update the parameter configuration to adapt the changes. The trained equilibrium mapping layer can rapidly derive traffic distribution from real-time ODs and background load, and map it to an optimal (or close-to-optimal) equilibrium graph.

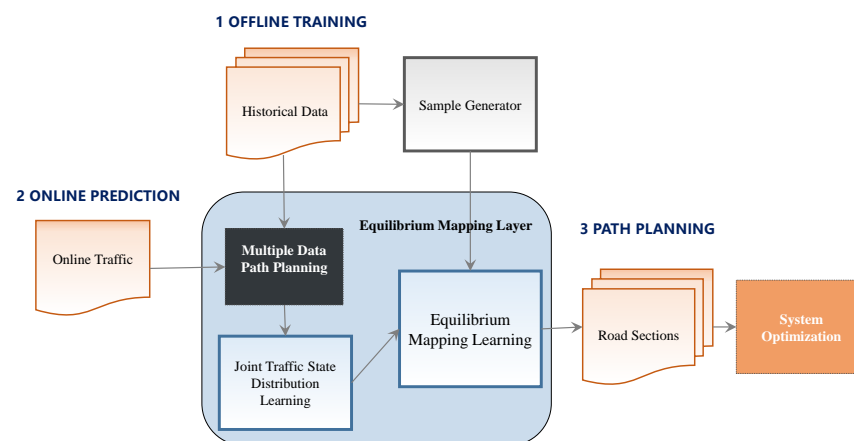


Figure 3. Hybrid control for path planning process based on data-driven deep learning.

*Equilibrium Mapping Learning:* To build the neural network for traffic graph learning, the equilibrium mapping layer can be implemented with multiple fully connected layers.

However, the mapping between traffic patterns and equilibrium distributions is complex, involving network traffic propagation and global implicit interaction. This requires a fully connected neural network with many layers of connection parameters, which are difficult to train in a reasonable time and limited samples [49]. The status of the traffic graph is complex and variable, so the interaction between sections should be dynamic as well. In particular, it has limitations in using the fixed adjacency matrix to model the spatial dependencies of ODs. Accordingly, we propose a multi-graph convolutional network that adopts an adaptive adjacency matrix [50] to capture the hidden spatial dependencies between traffic and topology configurations.

As shown in Figure 4, the inputs to the model contain the OD’s volume  $O \in \mathbb{R}^{n \times n}$  and the background load  $V \in \mathbb{R}^n$ . They are fused after multi-graph convolution resulting in a unique traffic pattern that corresponds to an equilibrium traffic graph. The equilibrium mapping layer efficiently learns the patterns in traffic and topology to achieve SO with higher performance. The traffic load graph  $G_v(R, \Lambda_v)$  is composed of the road sections  $R$  and topology relations  $\Lambda_v$ . The OD’s graph  $G_o(R, \Lambda_o)$  consists of  $R$  and semantic relations  $\Lambda_o$  of ODs. We use two separate feature graphs as basic components, with each component focusing on its own feature extraction and finally fusing them through a concatenation operation. The spatial dependencies of the HCN and AdaptiveHCN are based on the adjacent neighborhood  $\Lambda_v$  and OD semantic neighborhood  $\Lambda_o$ , respectively. The  $\Lambda_o$  is obtained by two learnable parameters  $E_o, E_d$ , where  $E_o$  is the origin embedding and  $E_d$  is the destination embedding. We obtain the OD semantic dependencies between the origin and destination, as shown in Equation (13).

$$\Lambda_o = \text{Softmax}(\text{Relu}(E_o \times E_d^\top)). \tag{13}$$

The Softmax is a probability distribution mapping function. And ReLU is applied to eliminate minor dependencies. The output  $\Lambda_o$  can be considered as a transfer matrix for implicit propagation based on ODs. Combined with the self-learning hidden graph dependencies, we propose the following multi-graph convolution operation:

$$Y^{(m)} = \Gamma^{(\text{MultiGraph})}([\Lambda_v V \Theta_v, \Lambda_o O \Theta_o] \cdot W^{(m)}). \tag{14}$$

After obtaining the latent encoding features of the OD and background load graphs, we use the multi-graph fusion mechanism to retain the original spatio-temporal features as completely as possible [51]. At the end, the derived feature graph is projected to the generated equilibrium graph via a fully connected layer. The trained equilibrium mapping layer can be efficiently assigned traffic online.

To train the input to output weights, we calculate the average error between the predicted traffic graph and the generated equilibrium graph. We expect the prediction results to be close to the ideal equilibrium graph by introducing the following loss function:

$$\text{Loss}(x, y) = \left\| \frac{1}{n_1} \sum_{r_i \in L_1} x_{r_i} C(r_i) - \frac{1}{n_2} \sum_{r_j \in L_2} y_{r_j} C(r_j) \right\|. \tag{15}$$

where  $x$  denotes the generated equilibrium traffic and  $y$  denotes the predicted assignment traffic. The  $n_1$  and  $n_2$  are the count of road sections contained in the OD path sets  $L_1$  and  $L_2$ , respectively. This loss is equivalent to the mean square error when  $L_1$  and  $L_2$  contain the same section.

*Path Planning based on ST-ETA:* As the background load and traveler evacuation volume change dynamically over time, the ST-ETA model should constantly update its traffic distribution to adapt the evolution, to guarantee the SO path planning from the origin at the current time step to the destination. The state correlations between the time steps are connected by the spatio-temporal characteristics of the traffic flow and the real-time OD trend features. Dynamic path decisions are stitched together by constantly giving the current step. The final output  $y$  represents the hypothesis of the travelers’ trajectories in

the network, interpreted as path planning based on the traffic equilibrium constraint. We adjust the road sections' rank according to the equilibrium topology configuration, which guides the path-planning method to use the potential traffic assignment sections for the routing decision. When a subject requests a path, the model performs path planning on the adjusted underlying graph, returning a path that meets the evacuation subject's demand and is consistent with system optimization.

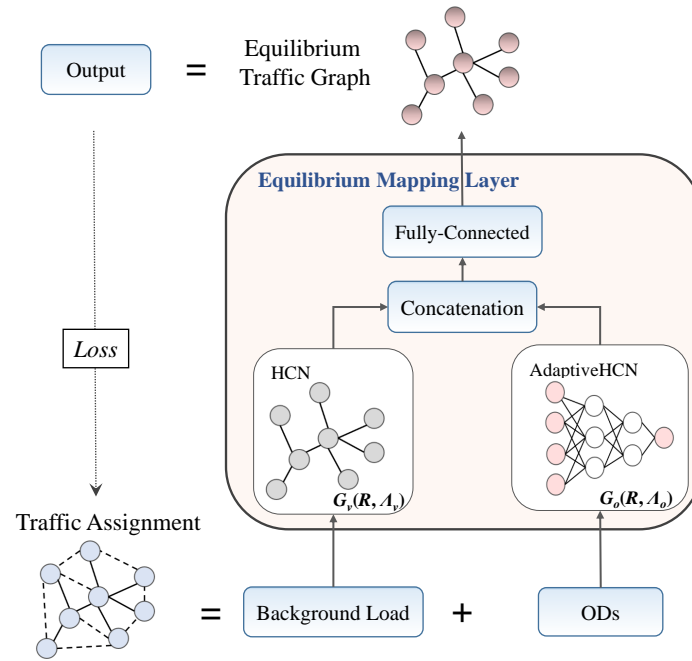


Figure 4. Equilibrium mapping based on adaptive multi-graph fusion.

### 5. Experimental Results and Analysis

The road network relied on for the experiments in this paper is derived from the map of Chengdu City provided by OpenStreetMap ([www.openstreetmap.org](http://www.openstreetmap.org), accessed on 28 December 2021), with 113,825 road sections and 81,371 nodes. The road network is contracted by edge aggregation to build 161,731 shortcuts. The latitude and longitude boundaries we used for the Chengdu City are [30.2775, 31.0328, 103.6767, 104.5578]. Considering that obtaining OD data of evacuation vehicles on the road network is limited, in our simulation experiments, we use the real-scene KDD CUP 2020 car-hailing datasets provided by Didi Chuxing ([gaia.didichuxing.com](http://gaia.didichuxing.com), accessed on 23 December 2021), to simulate the route data of evacuation vehicles for partial experimental verification. We scaled up in time granularity (1 h as a statistical unit) to approximate all travelers. The data range from 1 November to 30 November 2016.

*ODs Dataset:* The order dataset contains 7,062,959 OD records, each with a timestamp and geographic coordinates of the origin and destination. After matching the road network, the shortcuts were aggregated into 14,076 hierarchies to guide the OD semantic partition. The road network is also divided into  $35 \times 40$  (1400) geographical grids and the volume of ODs within the grids is aggregated. Since the end time of OD orders is not fixed, we take 1 h as the time step for prediction. For time-out orders are treated as completed in 1 h.

*Trajectories Dataset:* The total number of trajectories is 1,096,618,419 with each record containing a time stamp, vehicle ID, and geographical coordinates of the location. The trajectory points are collected at intervals of 2–4 s. The number of sections after mapping to the road network is 4036, leaving 2239 after further contraction.

*Road Section Impedance:* The road section impedance can be determined based on the relationship between evacuation time and traffic load. In this paper, the BPR function is

used as  $T(x_r, C_r) = t_r^0(1 + a \frac{x_r}{C_r})^\beta$ , where  $x_r$  is the traffic load on road section  $r$ ,  $C_r$  is the capacity, and  $t_r^0$  is the free-flow evacuation time. The parameters  $\alpha$  and  $\beta$  are taken as 0.15 and 4.5, respectively.

We choose three kinds of prediction errors to evaluate the performance of the model, MAE, RMSE, and accuracy, as in Equation (16):

$$\begin{aligned}
 MAE &= \frac{1}{m} \sum_{t=1}^m |y_t - x_t|, \\
 RMSE &= \sqrt{\frac{1}{m} \sum_{t=1}^m (y_t - x_t)^2}, \\
 Accuracy &= 1 - \frac{|y_t - x_t|}{x_t}.
 \end{aligned}
 \tag{16}$$

where  $y_t$  denotes the predicted value and  $x_t$  denotes the true value based on the OD volume, background load, or assigned traffic.  $m$  denotes the prediction period.

### 5.1. The Prediction Performance of OD Evacuation Volume and Background Load

In the experiments, we further verify the effect of hierarchy features on the prediction performance of existing methods. We compare the performance of hierarchy partition with grid partition using 12 h as the historical time window for training, as shown in Figure 5.

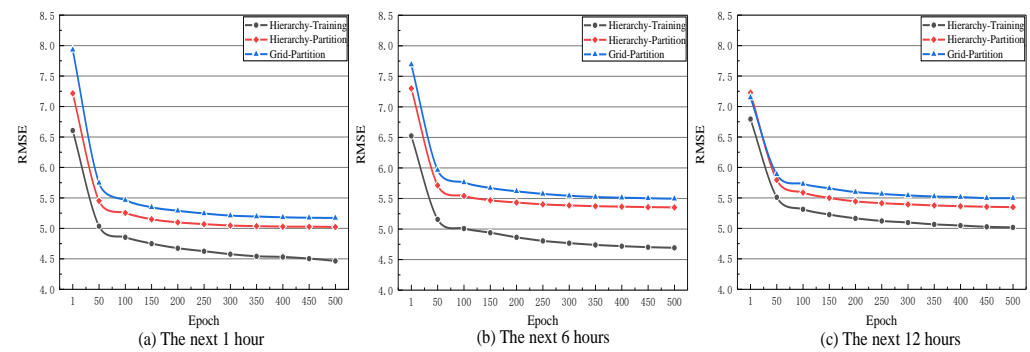


**Figure 5.** The prediction error of OD evacuation volume based on hierarchy and grid partitions.

The target is to predict potential evacuation demands for the next 1 h, 6 h, and 12 h. With increasing iterations of training, the RMSE becomes stable after 500 iterations. In general, the length of the prediction window has a direct impact on prediction performance. From Figure 5a, it can be seen that the model is best trained with a 1 h prediction window. In the first 500 iterations, the validation RME reached a minimum of 5.012. By extending the prediction scope to 12 h, the RMSE for three curves increases significantly, indicating that the prediction performance of the long-term prediction is lower than that of the short-term, which is more applicable to the need for short-term prediction in emergency scenarios. The small time scope allows the model to perform well, but the length of capturing the time series features is limited. In each subgraph, the overall RMSE under hierarchy partition is lower than that under grid partition, with a minimum value of 5.165 during 500 iterations. This is due to the fact that grid partition does not handle uneven distribution well, and using equal grids to aggregate OD data leads to a polarization in the dense and sparse data. This results in an over-generalized amount of OD evacuation after grid partition, and the evacuation features from one grid to another are not well-reflected. Therefore, the training performance of the traffic prediction under hierarchy partition is better than that of the grid partition.

In terms of background load prediction, the same 12 h time window is used to predict the background load for the next 1, 6, and 12 h, matching the dynamic OD evacuation volume. The experiments compare our proposed HCN with general graph convolution methods, respectively. The HC-LSTM employs spatial feature aggregation with HCN in each LSTM cell. Figure 6 shows the performance of GCN, HCN, and HC-LSTM on the

validation data. As the iterations increased in Figure 6, the RMSE under different modules leveled off gradually, and HC-LSTM outperformed the GCN and HCN in three prediction periods. In comparison to the baseline GCN, the average RMSE of HCN increases by 35.76%, while the HC-LSTM average RMSE increases by 48.28%. And HCLSTM uses spatio-temporal convolution, which improves by 19.49% relative to spatial convolution HCN. Similarly, the prediction performance of the models decreases as the scope of prediction window increases. The RMSE of HC-LSTM reaches a minimum of 26.63 for the next 1 h prediction. The experiments verified that the HCN outperforms the GCN due to the addition of hierarchy features that improve the fitting ability to traffic spatial relation.

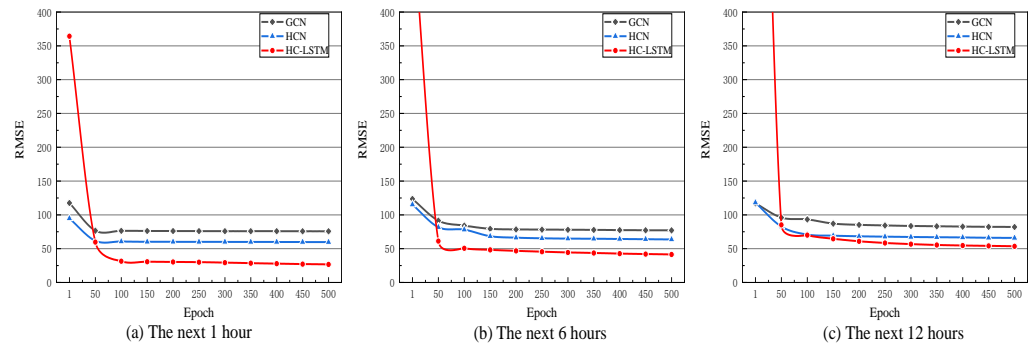


**Figure 6.** The background load prediction error under different convolution modules.

Therefore, by obtaining historical ODs and background load data of the traffic network, it is possible to make prediction for future traffic loads. Also, the experiments demonstrate that the performance of traffic prediction can be improved by mining the hierarchical semantic information of the road network.

### 5.2. The Availability and Timeliness of Equilibrium Traffic Assignment Prediction

To learn the correlation between the current traffic distribution with the optimally equilibrated traffic distribution map, and to achieve the prediction of the optimally equilibrated traffic distribution in new scenarios, the ST-ETA equilibrium mapping layer uses Equation (15) for model training. In the experiments of this paper, the optimal balanced flow distribution map sample data are generated by the equilibrium assignment method with SO as the optimization objective and solved by the F-W [52] method.

As can be seen from Figure 7a, the training RMSE, validation RMSE and MAE gradually decrease and level off over 500 iterations. The performance shown in Figure 7b can be achieved on the validation set after 500 training epochs, with an RMSE of 68.59, MAE of 41.34, and Accuracy of 78.60%. The horizontal coordinates of Figure 7c,d are shown in descending order by loads in the SO equilibrium distribution graph. Figure 7c illustrates the flow distribution between SO and ST-ETA for highly loaded sections with flows of 200–1500. It can be seen that ST-ETA captures the overall distribution pattern of SO well, but the flow loading is lower than the actual flow of SO. This suggests that ST-ETA merely captures the fact that high-traffic roads typically have a higher capacity to carry loads and can be used as critical evacuation roads in path planning. However, it cannot learn the maximum load carrying capacity of these critical roads. ST-ETA learns from multiple SO plans and "averages" several plans that are similar to the current scenario. When there exist SO plans that utilize certain roadways at or near-maximum capacity to accomplish evacuation, ST-ETA would allocate a small portion of the flow that exceeds the "average" capacity to the more critical and commonly used evacuation roads. This view can also be correspondingly corroborated from Figure 7d. This figure shows the comparison of two model flow distributions for the low-load road (0–200). Some low-load roads have slightly higher traffic volumes than the SO option. Certainly, this suggests that some travelers bear more costs in this evacuation (e.g., appropriately choosing a detour to a nearby roadway with lower loads). And the total system scheduling time increases accordingly. This is not

the absolute optimal balanced traffic distribution. But trying to achieve absolute optimality in a real large road network is unrealistic and the error is acceptable in terms of the total travel time comparison as seen in Section 5.3.

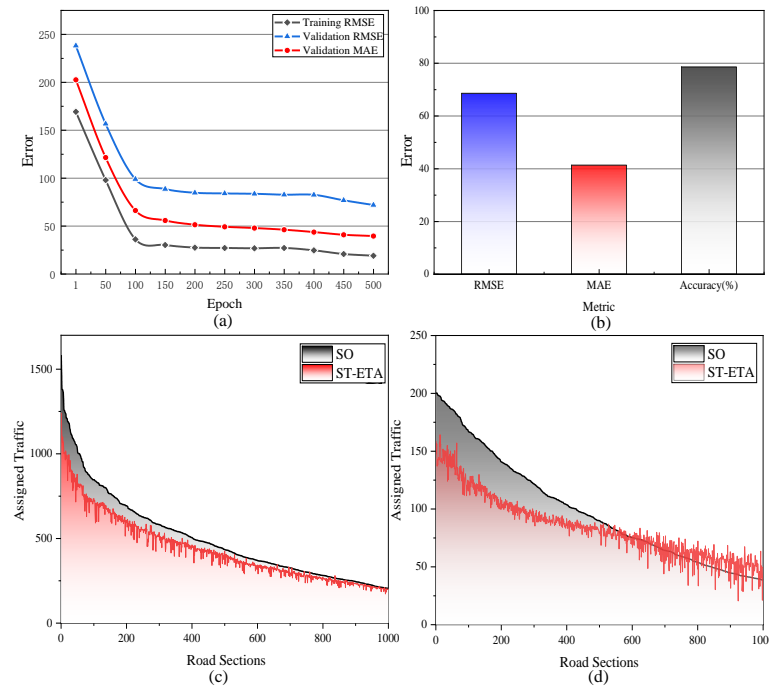


Figure 7. The prediction performance of ST-ETA.

In terms of model run times, we compare the data-driven method ST-ETA, which is mapped by the SO traffic assignment method, with the classical SO method MSA [11] and the F-W [52] method in terms of timeliness. The experiment uses the statistical OD evacuation volume and real-time calculated network capacity of the Chengdu road network from 13:00~14:00 on 1 November 2016. In Figure 8a, the MSA took 28 iterations to reach system optimization in 22,304.66 s, while the F-W required seven iterations in 5010.84 s. The ST-ETA was pre-trained using the neural network and took 14,257.14 s to perform 500 training iterations. The decision-making phase after training, as shown in Figure 8b, requires 843.93 s and 843.05 s for the FW and MSA allocation process based on an all-or-nothing policy, respectively. It cannot satisfy the demand of providing real-time path decision-making in emergency scenarios. The ST-ETA can provide a decision-making solution in only 101.51 s, which can effectively solve the problem of real-time decision-making for large-scale network path planning in emergencies.

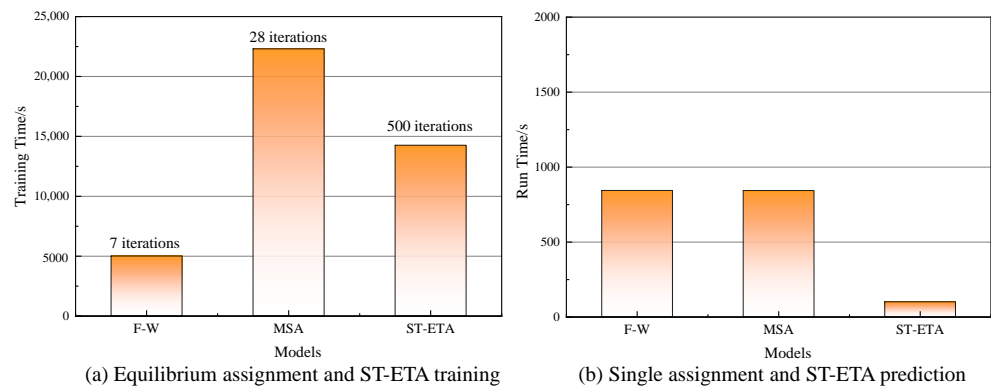


Figure 8. Comparison of the run time of different traffic assignment models.

### 5.3. The Other System Performance Based on Hybrid Control Path Planning

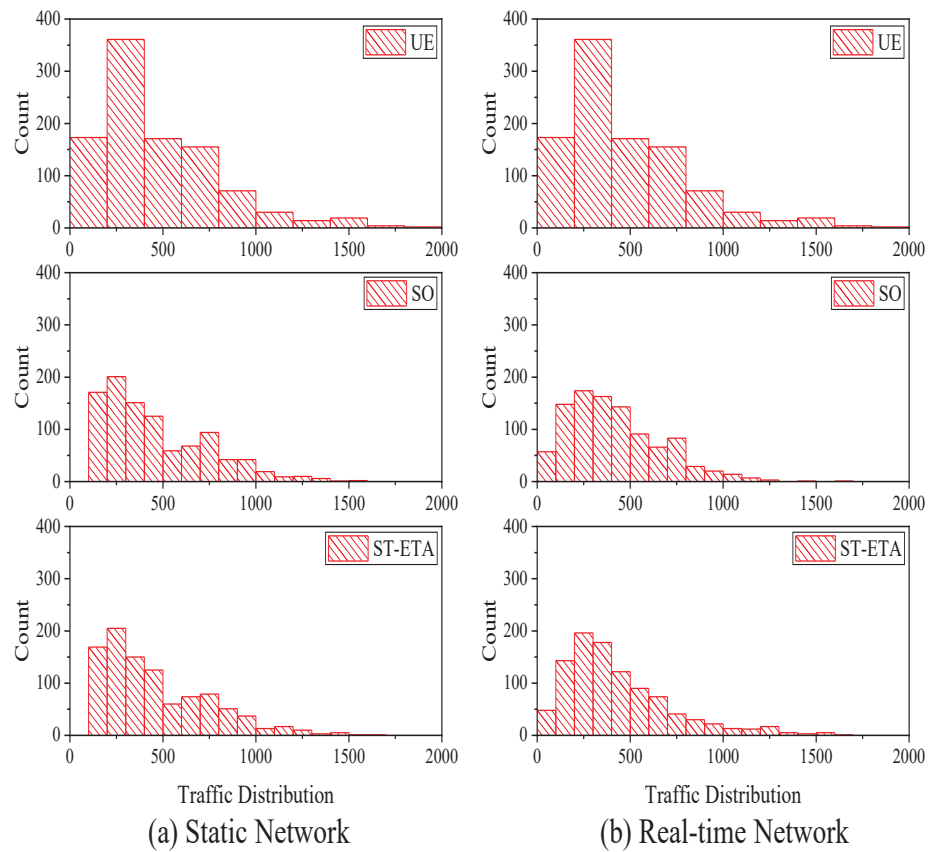
The ST-ETA prediction results in a traffic distribution that is close to the traffic equilibrium status, and it can be assumed that path planning according to this distribution will achieve SO. To better demonstrate the changes brought by hybrid control path planning to the traffic system, we have performed three traffic assignment models, namely UE, SO, and our proposed ST-ETA, based on static networks and real-time networks. In static networks, the traffic flows can be assigned according to the maximum capacity of the road network. The real-time network updates the network capacity periodically, considering the traffic load of the previous period.

Figure 9 illustrates the overall traffic distribution based on UE, SO, and ST-ETA for both static and real-time networks. The horizontal axis indicates the evacuation volume range and the vertical axis indicates the road sections count within that range. It can be seen that there are more high-traffic sections with traffic between 1000 and 2000 in UE. In contrast, SO and ST-ETA, which are aimed at system optimization, have fewer high-volume road segments and a slight increase in low-volume segments. This suggests that the adoption of SO and ST-ETA results in a more even loading of the roadway segments. This is more conducive to maintaining a steady state and coping with the recovery of emergency evacuation scenarios. Comparing Figure 9a,b, it can be seen that the SO and ST-ETA traffic distributions are close to each other in the static network scenario. This is due to the fact that ST-ETA is mapped based on the SO method. While in the dynamic network scenario, the ST-ETA histogram distribution is overall flatter, indicating a more balanced traffic distribution. Especially for the low and medium traffic sections, its road utilization is higher, which is more capable of alleviating the overall load of the high traffic sections. This proves that ST-ETA is better adapted to the balanced evacuation in the dynamic network of emergency scenarios.

Next, to visualize the system performance of ST-ETA under dynamic scenarios, we calculate the total evacuation time, average traffic load, and road utilization of the system with the three assignment models, as shown in Figure 10. UE has the highest total evacuation time. This is because its iteration only considers the traveler's self-interest to find the optimal path, and fails to consider the impact of the process that travels in real-time cooperation and competition among ODs on the road network state. In the dynamic network scenario, the average traffic load of UE is 215 and the road utilization is 62.66%. The average traffic load of SO decreased by 4.88% and road utilization increased by 8.57% compared to UE. ST-ETA had the lowest average traffic load of 201 and road utilization of 68.86%. This is consistent with the results of Figure 7c,d of Experiment 5.2. The improvement in ST-ETA road utilization is obtained at the expense of the total scheduling time. While the system travel time is comparable to SO, the error from the absolute system optimum is within acceptable limits.

Hybrid control path planning is used to advise multi-evacuation travelers to select paths in congested networks following the principle of system optimization. Specifically, ST-ETA predicts the volume of travelers' evacuation in advance to generate a traffic topology configuration. The hybrid control path planning prioritizes the road sections in the topology configuration during the routing decision, with the final path containing the maximum potential traffic. Figure 11 shows the paths using the Dijkstra shortest path planning method and the hybrid control path planning based on ST-ETA. Compared to the shortest path, the paths in Figure 11b use more road sections which come from the topology configuration obtained by ST-ETA prediction. Therefore, the hybrid control path planning contributes to the evolution of congested network to system optimization.





**Figure 9.** Comparison of traffic distributions of different assignment models. The (a) represent the traffic distribution in static , and the (b) represent the traffic distribution in real-time networks.

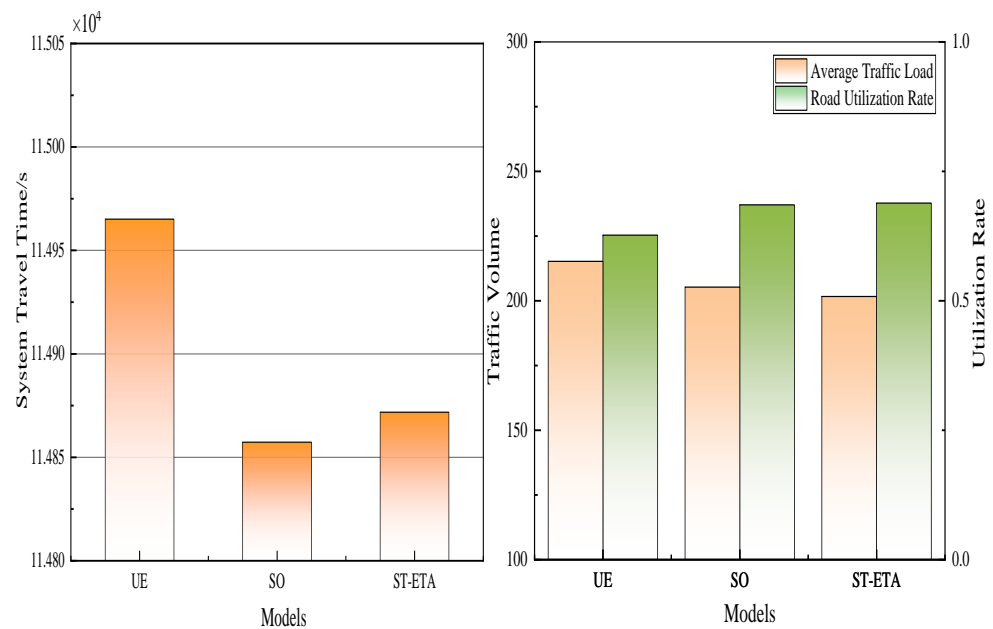


**Figure 10.** Comparison of system performance of traffic assignment models.

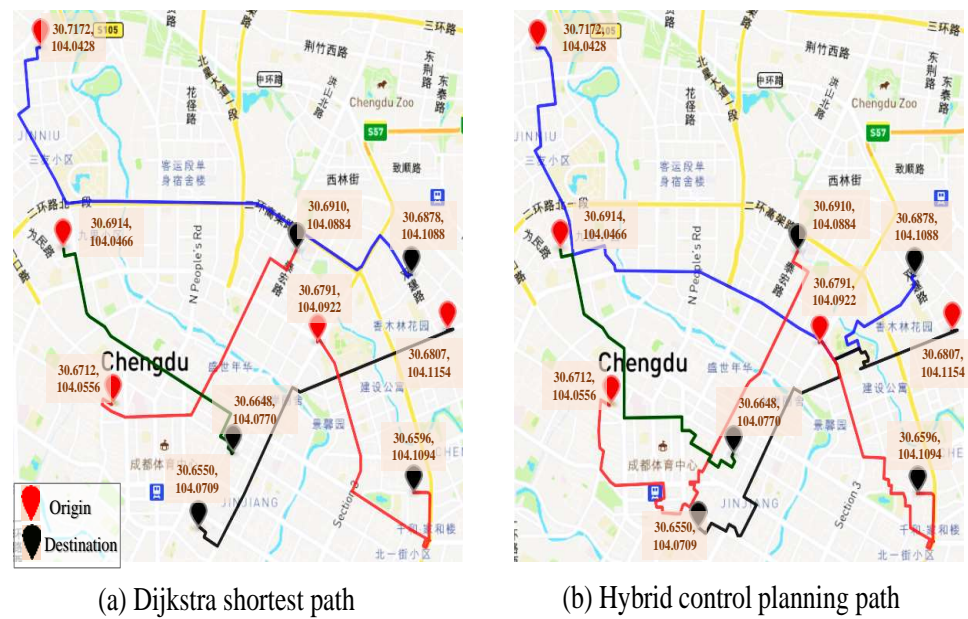


Figure 11. Comparison of hybrid control planning path and shortest path.

## 6. Conclusions and Future Work

The hybrid control path planning perceives the background traffic and evolution volume of the system to make individual path decisions. This paper first predicts the dynamic traffic load in large-scale networks using multidimensional features to provide a more accurate dynamic road network state for system-compatible emergencies. Then, its models macro and micro information using the adaptive multi-feature fusion technique, mapping the offline SO flow assignment method to generate equilibrium distribution graphs considering dynamic traffic states. Finally, the potential travel demand is assigned in a data-driven manner online in real time. Hybrid control path-planning techniques increase the diversity of path choices for evacuating travelers by sensing both macro and micro information, which is conducive to improving the capability of the transportation system to rapidly return to normality in emergencies. As this paper adopts the way of training the prediction and assignment model in advance, the network-wide dynamic traffic flow can be obtained in real time in the actual path-planning decision-making. Through the mapping of the assignment process without iteration, the algorithm can give the traffic assignment plan in real time, which is well adapted to the needs of rapid planning decisions in emergencies.

The current method applies to daily traffic and roads with temporary emergencies. It cannot be adapted to major disasters scenarios where the structure of the road network changes (e.g., earthquakes). This is because the forecasting method used involves the impact of the network's structural characteristics. Since ST-ETA cannot learn the maximum carrying capacity of the roadway, it allows roadway flows to be diverted when they exceed the average optimal distribution. While this alleviates the load on critical roads, it will result in a slight increase in the total evacuation time. In future work, a limit on the maximum load of the network can be added to the spatio-temporal network training to bring it closer to the SO optimal flow distribution. Otherwise, given the current state of emergency data and subject routes data collection, the model in this paper has some limitations at the data and validation level. The future work intends to collect and simulate more representative data of normal and non-normal scenarios, so as to further verify and compare the model performance under different scenarios in detail, and make more scenario-specific improvements to the model.

**Author Contributions:** Conceptualization, Z.Z. and M.C.; Methodology, Z.Z., Z.C., and M.C.; Software, Z.Z.; Writing—original draft, Z.Z.; Validation, Z.Z., Z.C. and M.C.; formal analysis, Z.C. and M.C.; investigation, Z.Z.; resources, Z.D.; data curation, M.C. and Z.D.; funding acquisition, Z.D. and Z.C. All authors have read and agreed to the published version of the manuscript.

**Funding:** This work is supported by the National Key R & D Program of China under Grant 2022YFF0503900, the Key R & D Program of Shandong Province under Grant 2021CXGC010104, the National Natural Science Foundation of China under Grant 62072016, Beijing Natural Science Foundation under Grant 4212016, and the Humanities and Social Sciences Foundation of the Ministry of Education under Grant 21YJA790009.

**Data Availability Statement:** The OpenStreetMap data presented in this study are available from <https://www.openstreetmap.org/> (OpenStreetMap, accessed on 28 December 2021). Restrictions apply to the availability of Didi Chuxing data. Data were obtained from <http://gaia.didichuxing.com/> (Didi Chuxing, accessed on 23 December 2021). These data are available from the authors upon contact.

**Conflicts of Interest:** The authors declare no conflicts of interest.

## Abbreviations

The main notations used in this paper.

### Notation

$G, G_{\uparrow}$	Topology of road network. Overlay graph of $G$ .
$R, r_i, R_{\uparrow}$	Road sections, with $ R  = n$ . The $i$ th road section in $R$ . Edges of $G_{\uparrow}$ .
$N, N_{\uparrow}$	Road intersections. Nodes of $G_{\uparrow}$ .
$A, D; A_{\uparrow}$	Adjacency matrix, Degree matrix of $G$ . Adjacency matrix of $G_{\uparrow}$ .
$\hat{A}, \hat{A}_{\uparrow}$	Normalized adjacency matrix of $A, A_{\uparrow}$ .
$C, \hat{C}$	Contraction correlation matrix. Normalized correlation matrix of $C$ .
$\hat{D}, \hat{D}_c, \hat{D}_{\uparrow}$	Degree matrix of $\hat{A}, \hat{C}, \hat{A}_{\uparrow}$ .
$V, v_r$	Traffic load of $R$ . Traffic load on link $r$ .
$O, o_r$	OD evacuation volume. Evacuation volume on link $r$ .
$T, t, m$	Coarse-grained time slice $T$ . Discrete time points $t, t \in T$ . Time interval.
ODs	The set of OD pairs for all travelers.
$L, l$	The paths corresponding to ODs. An OD path.
$F$	Traffic assigned probability distribution.
$\theta$	Chebyshev polynomial coefficient.
$\Theta$	Graph convolution parameter matrix.
$\Gamma$	Convolution filter.

## References

- Murray-Tuite, P.M. A comparison of transportation network resilience under simulated system optimum and user equilibrium conditions. In Proceedings of the 2006 Winter Simulation Conference, Monterey, CA, USA, 3–6 December 2006; IEEE: Piscataway, NJ, USA, 2006; pp. 1398–1405.
- Wardrop, J.G. Road paper. Some theoretical aspects of road traffic research. *Proc. Inst. Civ. Eng.* **1952**, *1*, 325–362. [\[CrossRef\]](#)
- Smeed, R.J.; Beckmann, M.; McGuire, C.B.; Winsten, C.B.; Koopmans, T.C. Studies in the Economics of Transportation. *Econ. J.* **1956**, *26*, 820–821. [\[CrossRef\]](#)
- Fisk, C. Some developments in equilibrium traffic assignment. *Transp. Res. Part B* **1980**, *14*, 243–255. [\[CrossRef\]](#)
- Dial, R. Equilibrium logit traffic assignment: Elementary theory and algorithms. In Proceedings of the 80th Annual Meeting of the Transportation Research Board, Washington, DC, USA, 7–11 January 2001; Volume 35
- Cova, T.J.; Johnson, J.P. A network flow model for lane-based evacuation routing. *Transp. Res. Part A Policy Pract.* **2003**, *37*, 579–604. [\[CrossRef\]](#)
- Xie, C.; Turnquist, M.A. Integrated evacuation network optimization and emergency vehicle assignment. *Transp. Res. Rec.* **2009**, *2091*, 79–90. [\[CrossRef\]](#)
- Liu, Y.; Luo, Z. A bi-level model for planning signalized and uninterrupted flow intersections in an evacuation network. *Comput.-Aided Civ. Infrastruct. Eng.* **2012**, *27*, 731–747. [\[CrossRef\]](#)
- Bayram, V.; Tansel, B.Ç.; Yaman, H. Compromising system and user interests in shelter location and evacuation planning. *Transp. Res. Part B Methodol.* **2015**, *72*, 146–163. [\[CrossRef\]](#)
- Pel, A.J.; Bliemer, M.C.; Hoogendoorn, S.P. A review on travel behaviour modelling in dynamic traffic simulation models for evacuations. *Transportation* **2012**, *39*, 97–123. [\[CrossRef\]](#)

11. Tong, C.; Wong, S. A predictive dynamic traffic assignment model in congested capacity-constrained road networks. *Transp. Res. Part B Methodol.* **2000**, *34*, 625–644. [\[CrossRef\]](#)
12. Florian, M.; Mahut, M.; Tremblay, N. Application of a simulation-based dynamic traffic assignment model. *Eur. J. Oper. Res.* **2008**, *189*, 1381–1392. [\[CrossRef\]](#)
13. Di Gangi, M. Modeling evacuation of a transport system: Application of a multimodal mesoscopic dynamic traffic assignment model. *IEEE Trans. Intell. Transp. Syst.* **2011**, *12*, 1157–1166. [\[CrossRef\]](#)
14. Zhang, T.; Ren, G.; Cheng, G.; Yang, Y.; Jin, M. A stochastic dynamic traffic assignment model for emergency evacuations that considers background traffic. *IEEE Intell. Transp. Syst. Mag.* **2021**, *14*, 206–220. [\[CrossRef\]](#)
15. Di Gangi, M.; Watling, D.; Di Salvo, R. Modeling evacuation risk using a stochastic process formulation of mesoscopic dynamic network loading. *IEEE Trans. Intell. Transp. Syst.* **2020**, *23*, 3613–3625. [\[CrossRef\]](#)
16. Bayram, V. Optimization models for large scale network evacuation planning and management: A literature review. *Surv. Oper. Res. Manag. Sci.* **2016**, *21*, 63–84. [\[CrossRef\]](#)
17. Peeta, S.; Ziliaskopoulos, A.K. Foundations of dynamic traffic assignment: The past, the present and the future. *Netw. Spat. Econ.* **2001**, *1*, 233–265. [\[CrossRef\]](#)
18. Hsu, Y.T.; Peeta, S. An aggregate approach to model evacuee behavior for no-notice evacuation operations. *Transportation* **2013**, *40*, 671–696. [\[CrossRef\]](#)
19. An, S.; Cui, N.; Li, X.; Ouyang, Y. Location planning for transit-based evacuation under the risk of service disruptions. *Transp. Res. Part B Methodol.* **2013**, *54*, 1–16. [\[CrossRef\]](#)
20. Goerigk, M.; Deghdak, K.; T'Kindt, V. A two-stage robustness approach to evacuation planning with buses. *Transp. Res. Part B Methodol.* **2015**, *78*, 66–82. [\[CrossRef\]](#)
21. Mahmassani, H.S. Dynamic network traffic assignment and simulation methodology for advanced system management applications. *Netw. Spat. Econ.* **2001**, *1*, 267–292. [\[CrossRef\]](#)
22. Ben-Akiva, M.; Bierlaire, M.; Koutsopoulos, H.N.; Mishalani, R. Real time simulation of traffic demand-supply interactions within DynaMIT. In *Transportation and Network Analysis: Current Trends: Miscellanea in Honor of Michael Florian*; Springer: Cham, Switzerland, 2002; pp. 19–36.
23. Mahut, M.; Florian, M.; Tremblay, N.; Campbell, M.; Patman, D.; McDaniel, Z.K. Calibration and application of a simulation-based dynamic traffic assignment model. *Transp. Res. Rec.* **2004**, *1876*, 101–111. [\[CrossRef\]](#)
24. Mao, X.; Yuan, C.; Gan, J.; Zhou, J. Optimal evacuation strategy for parking lots considering the dynamic background traffic flows. *Int. J. Environ. Res. Public Health* **2019**, *16*, 2194. [\[CrossRef\]](#)
25. Chiabaut, N.; Lopez, C.; Leclercq, L. Evaluation of the performance of an urban freight system using a multi-use-lane arterial. In Proceedings of the 95th Meeting of the Transportation Research Board, Washington, DC, USA, 10–14 January 2016.
26. Toqué, F.; Côme, E.; El Mahrsi, M.K.; Oukhellou, L. Forecasting dynamic public transport origin-destination matrices with long-short term memory recurrent neural networks. In Proceedings of the 2016 IEEE 19th International Conference on Intelligent Transportation Systems (ITSC), Rio de Janeiro, Brazil, 1–4 November 2016; IEEE: Piscataway, NJ, USA, 2016; pp. 1071–1076.
27. Cassidy, M.J.; Jang, K.; Daganzo, C.F. Macroscopic fundamental diagrams for freeway networks: Theory and observation. *Transp. Res. Rec.* **2011**, *2260*, 8–15. [\[CrossRef\]](#)
28. Xie, C.; Duthie, J. An excess-demand dynamic traffic assignment approach for inferring origin-destination trip matrices. *Netw. Spat. Econ.* **2015**, *15*, 947–979. [\[CrossRef\]](#)
29. Shi, H.; Yao, Q.; Guo, Q.; Li, Y.; Zhang, L.; Ye, J.; Li, Y.; Liu, Y. Predicting origin-destination flow via multi-perspective graph convolutional network. In Proceedings of the 2020 IEEE 36th International Conference on Data Engineering (ICDE), Dallas, TX, USA, 20–24 April 2020; IEEE: Piscataway, NJ, USA, 2020; pp. 1818–1821.
30. Liu, L.; Qiu, Z.; Li, G.; Wang, Q.; Ouyang, W.; Lin, L. Contextualized spatial-temporal network for taxi origin-destination demand prediction. *IEEE Trans. Intell. Transp. Syst.* **2019**, *20*, 3875–3887. [\[CrossRef\]](#)
31. Chu, K.F.; Lam, A.Y.; Li, V.O. Deep multi-scale convolutional LSTM network for travel demand and origin-destination predictions. *IEEE Trans. Intell. Transp. Syst.* **2019**, *21*, 3219–3232. [\[CrossRef\]](#)
32. Wang, Y.; Yin, H.; Chen, H.; Wo, T.; Xu, J.; Zheng, K. Origin-destination matrix prediction via graph convolution: A new perspective of passenger demand modeling. In Proceedings of the 25th ACM SIGKDD International Conference on Knowledge Discovery & Data Mining, Anchorage, AK, USA, 4–8 August 2019; pp. 1227–1235.
33. Zhang, J.; Zheng, Y.; Qi, D. Deep spatio-temporal residual networks for citywide crowd flows prediction. In Proceedings of the AAAI Conference on Artificial Intelligence, San Francisco, CA, USA, 4–9 February 2017; Volume 31.
34. Tian, Y.; Pan, L. Predicting short-term traffic flow by long short-term memory recurrent neural network. In Proceedings of the 2015 IEEE International Conference on Smart City/SocialCom/SustainCom (SmartCity), Chengdu, China, 19–21 December 2015; IEEE: Piscataway, NJ, USA, 2015; pp. 153–158.
35. Fu, R.; Zhang, Z.; Li, L. Using LSTM and GRU neural network methods for traffic flow prediction. In Proceedings of the 2016 31st Youth Academic Annual Conference of Chinese Association of Automation (YAC), Wuhan, China, 11–13 November 2016; IEEE: Piscataway, NJ, USA, 2016; pp. 324–328.
36. Wu, Z.; Pan, S.; Chen, F.; Long, G.; Zhang, C.; Philip, S.Y. A comprehensive survey on graph neural networks. *IEEE Trans. Neural Netw. Learn. Syst.* **2020**, *32*, 4–24. [\[CrossRef\]](#)

37. Li, Y.; Yu, R.; Shahabi, C.; Liu, Y. Diffusion convolutional recurrent neural network: Data-driven traffic forecasting. *arXiv* **2017**, arXiv:1707.01926.
38. Yu, B.; Yin, H.; Zhu, Z. Spatio-temporal graph convolutional networks: A deep learning framework for traffic forecasting. *arXiv* **2017**, arXiv:1709.04875.
39. Yu, B.; Lee, Y.; Sohn, K. Forecasting road traffic speeds by considering area-wide spatio-temporal dependencies based on a graph convolutional neural network (GCN). *Transp. Res. Part C Emerg. Technol.* **2020**, *114*, 189–204. [[CrossRef](#)]
40. Zhao, L.; Song, Y.; Zhang, C.; Liu, Y.; Wang, P.; Lin, T.; Deng, M.; Li, H. T-gcn: A temporal graph convolutional network for traffic prediction. *IEEE Trans. Intell. Transp. Syst.* **2019**, *21*, 3848–3858. [[CrossRef](#)]
41. Bai, J.; Zhu, J.; Song, Y.; Zhao, L.; Hou, Z.; Du, R.; Li, H. A3t-gcn: Attention temporal graph convolutional network for traffic forecasting. *ISPRS Int. J.-Geo-Inf.* **2021**, *10*, 485. [[CrossRef](#)]
42. Fang, S.; Zhang, Q.; Meng, G.; Xiang, S.; Pan, C. GSTNet: Global Spatial-Temporal Network for Traffic Flow Prediction. In Proceedings of the Twenty-Eighth International Joint Conference on Artificial Intelligence (IJCAI-19), Macao, China, 10–16 August 2019 ; pp. 2286–2293.
43. Dial, R.B. A path-based user-equilibrium traffic assignment algorithm that obviates path storage and enumeration. *Transp. Res. Part B Methodol.* **2006**, *40*, 917–936. [[CrossRef](#)]
44. Schaub, M.T.; Delvenne, J.C.; Lambiotte, R.; Barahona, M. Multiscale dynamical embeddings of complex networks. *Phys. Rev. E* **2019**, *99*, 062308. [[CrossRef](#)]
45. Kipf, T.N.; Welling, M. Semi-supervised classification with graph convolutional networks. *arXiv* **2016**, arXiv:1609.02907.
46. Ying, Z.; You, J.; Morris, C.; Ren, X.; Hamilton, W.; Leskovec, J. Hierarchical graph representation learning with differentiable pooling. In Proceedings of the Advances in Neural Information Processing Systems, Montreal, Canada, 3–8 December 2018; Volume 31.
47. Geisberger, R.; Sanders, P.; Schultes, D.; Delling, D. Contraction hierarchies: Faster and simpler hierarchical routing in road networks. In Proceedings of the Experimental Algorithms: 7th International Workshop, WEA 2008, Provincetown, MA, USA, 30 May–1 June 2008 ; Springer: Berlin/Heidelberg, Germany , 2008; pp. 319–333.
48. Guo, S.; Lin, Y.; Feng, N.; Song, C.; Wan, H. Attention based spatial-temporal graph convolutional networks for traffic flow forecasting. In Proceedings of the the AAAI Conference on Artificial Intelligence, Honolulu, HI, USA, 27 January–1 February 2019; Volume 33, pp. 922–929.
49. Wang, M.; Cui, Y.; Xiao, S.; Wang, X.; Yang, D.; Chen, K.; Zhu, J. Neural network meets DCN: Traffic-driven topology adaptation with deep learning. *Proc. ACM Meas. Anal. Comput. Syst.* **2018**, *2*, 1–25. [[CrossRef](#)]
50. Wu, Z.; Pan, S.; Long, G.; Jiang, J.; Zhang, C. Graph wavenet for deep spatial-temporal graph modeling. *arXiv* **2019**, arXiv:1906.00121.
51. Xu, K.; Li, C.; Tian, Y.; Sonobe, T.; Kawarabayashi, K.i.; Jegelka, S. Representation learning on graphs with jumping knowledge networks. In Proceedings of the 35th International Conference on Machine Learning, PMLR, Stockholm, Sweden, 10–15 July 2018; pp. 5453–5462.
52. Li, F.; Wang, S. Determining route traffic flows for traffic assignment problem with Frank-Wolfe algorithm. In Proceedings of the IEEE Proceedings, Intelligent Vehicles Symposium, Las Vegas, NV, USA, 6–8 June 2005; IEEE: Piscataway, NJ, USA, 2005; pp. 669–673.

**Disclaimer/Publisher’s Note:** The statements, opinions and data contained in all publications are solely those of the individual author(s) and contributor(s) and not of MDPI and/or the editor(s). MDPI and/or the editor(s) disclaim responsibility for any injury to people or property resulting from any ideas, methods, instructions or products referred to in the content.